On the dual nature of lichen-induced rock surface weathering in contrasting micro-environments

Title

On the dual nature of lichen-induced rock surface weathering in contrasting micro-environments

Authors

Joana Marques[a,b,c*], João Gonçalves[a,b], Cláudia Oliveira[a,b], Sergio E. Favero-Longo[d], Graciela Paz-Bermúdez[c], Rubim Almeida[a,b], Beatriz Prieto[e]

[a]CIBIO, Centro de Investigação em Biodiversidade e Recursos Genéticos, Campus Agrário de Vairão, 4485-661 Vairão, Portugal.

[b]Departamento de Biologia, Faculdade de Ciências, Universidade do Porto, Edifício FC4, Rua do Campo Alegre s/n, 4169-007 Porto, Portugal.

[c]Escola Universitaria de Enxeñeria Forestal, Universidade de Vigo, Campus Universitario A Xunqueira s/n, 36005 Pontevedra, Spain.

[d]Dipartimento di Scienze della Vita e Biologia dei Sistemi, Università degli Studi di Torino, Viale Mattioli 25 10125 Torino, Italy.

[e]Departamento de Edafología y Química Agrícola, Facultad de Farmacia, Universidad de Santiago de Compostela, 15782 Santiago de Compostela, Spain.

* Corresponding author. E-mail address: joanamarques@cibio.up.pt. Full postal address: CIBIO, Campus Agrário de Vairão, 4485-661 Vairão, Portugal. Phone number: (00351) 969019556.

Abstract

Contradictory evidence from biogeomorphological studies has increased the debate on the extent of lichen contribution to differential rock surface weathering in both natural and cultural settings. This study, undertaken in Côa Valley Archaeological Park, aimed at evaluating the effect of rock surface orientation on the weathering ability of dominant lichens. Hyphal penetration and oxalate formation at the lichen-rock interface were evaluated as proxies of physical and chemical weathering, respectively. A new protocol of pixel-based supervised image classification for the analysis of periodic acid-Schiff stained cross-sections of colonized schist revealed that hyphal spread of individual species was not influenced by surface orientation. However, hyphal spread was significantly higher in species dominant on north-west facing surfaces. An apparently opposite effect was noticed in terms of calcium oxalate accumulation at the lichen-rock interface, detected by Raman spectroscopy and complementary X-ray microdiffraction on south-east facing surfaces only.

These results suggest that lichen-induced physical weathering may be most severe on north-west facing surfaces by means of an indirect effect of surface orientation on species abundance, and thus dependent on the species, whereas lichen-induced chemical weathering is apparently higher on south-east facing surfaces and dependent on micro-environmental conditions, giving only weak support to the hypothesis that lichens are responsible for the currently observed pattern of rock-art distribution in Côa Valley. Assumptions about the drivers of open-air rock-art distribution patterns elsewhere should also consider the micro-environmental controls of lichen-induced weathering, to avoid biased measures of lichen contribution to rock-art deterioration.

Keywords

Biodeterioration, Biogeochemistry, Biomineralization, Raman spectroscopy, XRMD, Image analysis, Schist

Introduction

The last three decades have been extremely rich in contributions to the knowledge of the various aspects of lichen-induced rock weathering, as seen by the number of reviews available (Adamo & Violante 2000, Chen et al. 2000, Seaward 2015, St. Clair & Seaward 2004). Alternative approaches to this subject have been focusing on: i) identifying individual species and species assemblages colonizing rock surfaces and making assumptions on their impact based on previous knowledge about their ecological requirements (e.g. Carballal et al. 2001); ii) determining the climatic constraints and habitat preferences of colonizing species based on field observations (e.g. Steinbauer et al. 2013, Viles & Cutler 2012) or controlled experiments (Adamson et al. 2013, Carter & Viles 2003, Kidron & Termina 2010) thus contributing to the knowledge of environmental factors that are also important for rock conservation; iii) detecting geophysical and geochemical changes at the lichen-rock interface associated with the growth of individual species including the occurrence of organic and mineral by-products of lichen activity (e.g. Arocena et al. 2007, Favero-Longo et al. 2005); iv) addressing the influence of human activities on such changes (e.g. Cámara et al. 2015) and v) developing methods to quantify the weathering rates induced by individual species or by a limited set of the most representative ones on the

surface of interest (e.g. Aghamiri & Schwartzman 2002, Bartoli et al. 2014, Gazzano et al. 2009a, b, McIlroy de la Rosa et al. 2014).

The majority of work has been applied at characterizing the biodeterioration of a range of stonework in Europe and only sporadically in other regions of the globe. Few papers have dealt with the relationship between lichen growth and the weathering of schist (Aghamiri & Schwartzman 2002, Cann et al. 2012, Galvan et al. 1981, Fry 1924, 1927, Sanders et al. 1994) despite the increasing demand of schist as a building stone.

The processes of schist weathering, including those induced by lichen activity, are a primary concern in the Côa Valley Archaeological Park (Vila Nova de Foz Côa, north-east Portugal) where one of the world's most important sets of Prehistoric rock-art is located, almost invariably on schistose surfaces. Efforts are being made there to understand the weathering dynamics acting on the schist outcrops that support the rock-art, integrating biological, geophysico-chemical and environmental data in order to prevent major damages to the engraved surfaces (Aubry et al. 2012). There is general consensus about the combination of physical (mechanical) and chemical changes brought about by lichens to rock surfaces but the extent and relative contribution of their weathering action is a fundamental, yet still unanswered question, both in the Côa Valley and in the field of rock-art conservation in general. Adding to the debate over the threats of lichen-induced processes is the contradictory evidence for lichen protection of rock surfaces against other deteriogenic agents (Carter & Viles 2005, McIlroy de la Rosa et al. 2013).

Recently, Aubry et al. (2012) suggested that aspect-related differences in the extent of lichen (and bryophyte) colonization of vertical schist surfaces in the Côa Valley could be partly responsible for the differential weathering of those surfaces and resulting pattern of rock-art distribution in the Côa Valley, which is currently more concentrated at south-east facing than at

92 north-west facing slopes (Fernandes 2012). Provided that the interaction between lichens and the
93 rock surface is species-dependent (e.g. Favero-Longo et al. 2005), a key uncertainty in the
94 assumptions on the relationship between lichen colonization and rock weathering is precisely in
95 the way that lichen species act under different weathering environments. Studies aimed at
96 evaluating the response of individual species to changes in environmental conditions have
97 typically demonstrated a shift in oxalate production (thus in the biodeteriorative action) in
98 response to environmental variation (Caneva 1993, Edwards et al. 1995, Prieto et al. 2000). The
99 extreme environments of cold and hot deserts have been particularly interesting for research (e.g.
100 Wierzchos et al. 2013) since, besides acting differently in distinct weathering contexts, species
101 are also expected to change their performance under the influence of environmental change.
102 However, although useful first approximations, the existing studies commonly assume species
103 neutrality, with substrate and climate as the primary controls. As a result, knowledge about
104 lichen-induced rock weathering is mostly based on static views of the influence of
105 environmental, geological or climatic parameters such as rock porosity, permeability and
106 mechanical properties, or temperature, solar radiation and humidity.
107 The variation of the diversity and composition of lichen assemblages with rock surface
108 orientation is a well-known phenomenon in both natural and cultural contexts (Adamson et al.
109 2013) as orientation acts as a proxy of those environmental variables, mainly temperature and
110 humidity, which affect the structure and dynamics of saxicolous lichen communities. Some
111 components of that variation in the Côa Valley have been previously addressed from an
112 ecological perspective (Marques et al. 2014).
113 The present study directly assessed the effect of rock surface orientation on lichen-induced
114 physical and chemical weathering in order to determine the contribution of lichen action to

115 differential rock weathering in the Côa Valley Archaeological Park. Hyphal penetration and
116 calcium oxalate formation at the lichen-rock interface were confidently assumed as proxies for
117 physical and chemical weathering, respectively. Although how much hyphae penetrate through
118 existing pores and fissures or actively produce discontinuities in the rocks is not definitely clear,
119 microscopical observations have shown that penetrating hyphae induce mineral breakage and
120 rock surface disaggregation by mechanical action (Ascaso & Wierzchos 1995, Favero-Longo et
121 al. 2005). The close relationship between the chemical composition of colonized rocks and the
122 type of oxalates accumulating immediately beneath or within the thalli of some lichen species
123 have generally indicated an involvement of the mycobiont-secreted oxalic acid in lichen-induced
124 chemical weathering of rock substrata (Adamo & Violante 2000 with refs. therein).

125 **Material and methods**

126

127 The study area

128

129 The Côa Valley Archaeological Park is a UNESCO world heritage site located in the confluence
130 of River Côa with River Douro, approximately 200 km upstream of the mouth of the Douro, in
131 the city of Porto (Portugal). Lithology in this part of the Côa Valley is dominated by meta-
132 sedimentary rocks of the schist-greywacke complex ranging in age from the Precambrian to the
133 Ordovician. River Côa and its tributary streams have cut deeply through the schist and
134 greywacke basement, taking advantage of pre-existing major faults roughly NE-SW oriented
135 (Aubry et al. 2012) and forming numerous steep-walled valleys that play a major influence on
136 regional landscape. A special feature resulting from the down-cutting of the Côa Valley is the
137 occurrence of massive vertical schist surfaces arranged in layers along the valley's slopes, which

have been gradually exposed by rock toppling, i.e. a sequence of gravity-induced block displacement after splitting of vertically orientated joints, along the schistosity plane. Climate is predominantly dry meso-Mediterranean, sheltered from the Atlantic influence by mountains to the north and the west, but thermo-Mediterranean microclimates are usually produced in the bottom of the valleys, where temperature is frequently above 40°C in late spring and summer (June-August), daily thermal amplitudes may reach 10º to 15º C and mean annual precipitation is often below 300 mm (Fernandes 2012).

Geological and mineralogical characterization of the studied lithotype

The target lithotype is a relatively low-grade metamorphic (greenshist facies) phyllite consisting of thin alternating layers of whitish psammitic and dark pelitic components (Aires et al. 2011, Búrcio 2004, Sousa 1982). The psammitic component is sometimes more abundant and the rock is then classified as a metaquartzwacke instead of a phyllite. For a matter of simplicity, this phyllite-metaquartzwacke sequence will be addressed under the broad term schist. This schist is mainly composed of quartz, sericite and/or muscovite, chlorite and biotite minerals, as well as plagioclase feldspars (mostly albite) in variable amounts depending of the psammitic contribution. Calcite is usually present in the matrix of these rocks in sufficient amounts to produce effervescence when treated with dilute hydrochloric acid. Magnetite and, more sporadically, pyrite crystals are present in both the psammitic and pelitic levels as accessory constituents (Sousa 1982). Additional accessory minerals including illite, kaolinite, montmorillonite, graphite, turmaline, zircon, apatite, epidote, hematite, leucoxene and alkali feldspars, such as microcline and orthoclase, were detected by polarized light (petrographic)

161 microscopy and X-ray diffraction (Aires et al. 2011, Búrcio 2004, Gomes & Almeida 2003,
162 Sousa 1982). The general strike of the target fracture/joint surfaces is NE-SW, which is sub-
163 parallel to the NNE-SSW sinistral strike-slip fault system that crosses the study area and formed
164 by the same tectonic stress (Aubry et al. 2012). The plane of schistosity is consistently vertical
165 and oriented subperpendicular to the fracture/joint surfaces.
166
167 Microclimatic characterization of vertical schist surfaces in the Côa Valley
168
169 To characterize the thermal and hydric contrasts of opposite slopes in the Côa Valley,
170 Hygrochron iButton data-loggers (Maxim Integrated Products Inc., Sunnyvale (CA), USA) were
171 placed on 12 vertical schist surfaces of varying orientations. The results were then grouped in the
172 two aspect classes of interest for this study: north-west (NW) and south-east (SE). Data-loggers
173 were synchronized and set to record both temperature (ºC) and relative humidity (%), at hourly
174 or half-hourly intervals during a 3-year period from late September 2010 to late September 2013.
175
176 Target species
177
178 The study dealt with the physical and chemical weathering driven by four locally-common
179 lichens: *Aspicilia contorta* subsp. *hoffmanniana* S. Ekman & Fröberg (*Aspicilia hoffmanniana*
180 hereafter), *Caloplaca subsoluta* (Nyl.) Zahlbr., *Lecanora pseudistera* Nyl. and *Peltula euploca*
181 (Ach.) Poelt. Taxa selection was based on higher frequency and abundance (cover) on the
182 vertical schist surfaces of the Côa Valley Archaeological Park (Marques et al. 2014). *Aspicilia*
183 *hoffmanniana* is a crustose lichen varying in colour from greenish-grey in shaded NW facing

surfaces to light brown in exposed SE facing surfaces, where it is more abundant. *Caloplaca subsoluta* is a deep orange coloured crustose species that is common on siliceous rocks throughout the Mediterranean. In the Côa Valley it was found equally abundant on the vertical schist surfaces of the two opposing slopes. *Lecanora pseudistera* is a white crustose species proliferating on NW facing surfaces, although it can also be found less abundantly on SE facing schist surfaces. *Peltula euploca* is a widespread squamulose epilith characteristic of the rain-track communities of vertical schist surfaces and exclusive of SE facing exposures (Marques et al. 2014). Each squamule is attached to the substrate by a central umbilicus and its lower surface is pale to dark brown. The algal partner is *Trebouxia* spp. in the three crustose lichens and unicellular cyanobacteria (*Chroococcidiopsis* spp.) in *Peltula euploca*. The three crustose lichens are able to reproduce sexually, although *Aspicilia hoffmanniana* is most frequently sterile. *Peltula euploca* is often fertile in the study area but its characteristic mode of dispersal is through vegetative propagules (soredia). Secondary compounds in *Aspicilia hoffmanniana* are either lacking or include only aspicilin. *Caloplaca subsoluta* produces anthraquinones. The major secondary metabolites produced by *Lecanora pseudistera* are atranorin and 2'-O-methylperlatolic acid. *Peltula euploca* lacks secondary metabolites.

Sampling strategy and in-field sample collection

Colonized rock samples, with lichen thallus kept intact, were taken at random from non-engraved NW and SE facing schist surfaces, located at representative rock-art sites, namely Canada do Amendoal, Foz do Côa, Quinta das Tulhas, Vale do Forno and Vale de José Esteves, and are therefore very similar to the surfaces bearing rock-art in terms of their macro- and micro-

environmental constraints. Since *Peltula euploca* is virtually exclusive of SE facing surfaces, appropriate samples of rock colonized by this particular species could only be found and collected at SE. Uncolonized rock samples were also taken from the source outcrops to be used as controls. The use of bare-rock controls is a necessary condition for isolating the lichen-induced effects from the ones induced by other weathering agents (either biotic or abiotic). The collected samples were cut perpendicular to the colonized or previously exposed surface, up to a depth of 3 to 4 cm and width of 5 cm, with an Isomet 1000 Precision Saw (Buehler, Düsseldorf, Germany). The surfaces of the resulting cross-sections were polished with sandpaper attached to an Ecomet 3000 (Buehler, Düsseldorf, Germany) polisher machine. Nine replicates were prepared for each combination of species vs orientation, and respective control (uncolonized) in order to evaluate if weathering associated with lichen colonization differs from the weathering produced on identical but lichen-free surfaces. Three subsets of three replicates each were taken from the initial sample set, and processed accordingly for Periodic acid-Schiff (PAS) staining, X-ray microdiffraction and FT-Raman spectroscopy. Almost all samples had been included in polyester resin (*Recapoli* 2196 styrene and phthalic anhydride, Methyl Ethyl Ketone peroxide as catalyst) before cutting, to avoid excessive loss of material due to the fragile nature of the schist samples, except for those used in Raman analysis, since resin inclusion would preclude from taking measures directly on the lichen thallus.

Periodic acid-Schiff staining

This procedure aimed at highlightingthe Hyphal Penetration Component (HPC) of the target lichen species, as a proxy of lichen-induced physical weathering, following Favero-Longo *et al.*

(2005). Microphotographs of the stained cross-sections were then acquired at a ×10 magnification using a Nikon SMZ1000 stereomicroscope equipped with a Nikon DS Fi1 digital camera, at three random locations of each cross-section. Data on the depth of hyphal penetration was obtained by visual inspection of all hyphal bundles highlighted in the stained cross-sections under the same stereomicroscope. The mean and the maximum of measured data were calculated for each species at different aspects to provide the average and maximum depth of hyphal penetration sensu Favero-Longo *et al*. (2011).

In order to quantify the extent of hyphal penetration, as well as the size of other important weathering-related features (*e.g.* weathering rind), the acquired images were submitted to a new protocol of pixel-based supervised classification using colour and texture features, which can be described briefly as follows: 1) Image pre-processing in ImageJ (http://imagej.nih.gov/ij/), including the resize of original images to 40% of the initial size using bilinear resampling (to increase computation speed and efficiency) and contrast and sharpening enhancement to allow a better discrimination of the HPC and weathering rind (when present), from the rock core; 2) Feature extraction, including a total of 162 texture features based on run-length, co-occurrence, image histogram and gradient matrices in MaZda (http://www.eletel.p.lodz.pl/programy/mazda/) and colour features based on several colour spaces namely RGB, HIS, YUV, YIQ and XYZ using 'adimpro' package (Polzehl & Tabelow 2007) in R; 3) Generation of training input data in ImageJ, by manually assigning points (i.e., XY coordinates of pixels) in the original images to the corresponding structures of interest, namely 'lichen thallus', 'hyphae', 'weathering rind' and 'rock core'; 4) Combination of the extracted features and training data, to calibrate a Random Forest (RF) classifier (Breiman 2001, Liaw & Wiener 2002) in R with 'ntree'= 200, 'mtry'= 6, 'nodesize'= 5 and the remaining parameters kept as default; the feature set included only a

253 reduced subset containing the 20 top colour and texture features according to their relative
254 predictive importance (Boulesteix et al. 2012, Oppel et al. 2009); 5) Evaluation of classifier's
255 performance through Monte-Carlo cross-validation (Xu et al. 2004) with 70% for training and
256 30% for testing and a total of 100 replicates; 6) Prediction of the labels of the structures of
257 interest for the whole image, using the RF classifier with highest overall test accuracy. The
258 extent of the HPC and weathering rind (given in mm^2) in each sample are among the descriptive
259 statistics retrieved by the classifier.
260
261 FT-Raman spectroscopy
262
263 Spectroscopic analyses were performed in three locations of each colonized schist sample: 1) the
264 upper layer (cortex) of the lichen thalli as in Prieto et al. (2000); 2) the surface of the rock in
265 contact with the lichen thallus, named lichen-rock interface (Ascaso et al. 1976), where mineral
266 neoformation, if taking place at all, is most likely to be due to lichen-rock interactions; and 3) the
267 rock interior (at least 2 cm away from the surface) which is used as a specific control for each
268 sample since lichen-induced oxalate formation is assumed not to reach such deeper areas beneath
269 the lichen-rock interface (Adamo & Violante 2000). Control FT-Raman spectra were also
270 recorded on non-colonized schist samples collected from the same schist outcrops, including 1)
271 the exposed surface (taken from the top as in colonized samples); 2) a 5 mm deep virtual
272 interface; and 3) the rock interior. A Bruker RFS 100/S FT-Raman spectrometer was used with a
273 Nd:YAG laser operating at 1064 nm as the excitation light source and a resolution of 4 cm^{-1}.
274 Spectral data were acquired after 1024 laser scans of 20 mW in lichen thallus, to minimize lichen
275 damage, and 64 laser scans of 250 mW in rock interior and lichen-rock interface.

276

277 X-ray microdiffraction (XRMD)

278

279 XRMD measurements were performed on an Empyrean (PANalytical, Almelo, The Netherlands)
280 diffractometer, equipped with a five-axis Chi-Phi-x-y-z stage goniometer, a copper sealed
281 anticathode X-ray tube (*Empyrean Tube Cu Lff Hr*) and a PIXcel^{3D} (PANalytical, Almelo, The
282 Netherlands) X-ray detector. Each sample was first submitted to a set of five random line scan
283 readings along the polished cross-section in order to obtain a preliminary depth profile of the
284 mineralogical composition of the studied schist. Yet no significant differences were detected
285 between the surface of the sample and its interior so priority was given to the lichen-rock
286 interface as in FT-Raman spectroscopy. The final measurements are based on ten random
287 readings along the lichen-rock interface. Bragg angles were scanned between 4 and 47º, with
288 steps of 0.02º (12 minutes time length) for exploratory measurements and between 3.5 and 60º,
289 with steps of 0.02º (2 hours time length) for the final measurements, with a laser diameter of 0.6
290 mm.

291

292 Statistical analysis

293

294 The effects of species and orientation on the depth and extent of the Hyphal Penetration
295 Component (HPC) was tested by means of two-way analysis of variance (ANOVA) and post-hoc
296 Tukey HSD for pair-wise comparisons with 'agricolae' package (de Mendiburu 2013) in R.
297 ANOVA's assumption of normality of residuals was checked graphically using qq-plots and that
298 of homoscedasticity tested by means of the Levene test, also in R.

Results and discussion

Lichen-induced physical weathering

The pattern of hyphal penetration into the rock substrate is highly influenced by the characteristics of the rock (Sanders *et al.* 1994) since hyphae tend to follow paths of least resistance. Depth of hyphal penetration of the four lichens analysed was on average 3.4 mm in samples coming from NW facing surfaces (n= 12), 4.6 mm in samples coming from SE facing surfaces (n= 9), and varied between 0.1 to 37 mm when considering all samples. Maximum depth of hyphal penetration is apparently higher at SE than at NW facing surfaces (Table 1). However, within sample variation, as depicted by the standard-deviation, was extremely high and there was no statistically significant effect of orientation or species in the depth of hyphal penetration. Additionally, although maximum depth of hyphal penetration detected among the analysed samples was 37 mm (in *Aspicilia hoffmanniana* from SE facing surfaces), hyphal bundles frequently reached the lower extremity of the samples, which were roughly between 30 and 40 mm long, and measure of real maximum depth of penetration could not be accurately estimated. As suggested by previous works (e.g. Favero-Longo *et al.* 2005, Wierzchos & Ascaso 1996, 1998) schistose rocks may be susceptible to greater lichen-induced weathering than igneous rocks due to their higher predisposition to break and the easier progression of hyphae along the planes of weakness, parallel to the schistosity (Fig. 1). Additional planes of weakness come from the intense tectonically-related fracturing that characterizes the studied rock. One feature observed in almost every sample, and also commonly referred in literature (e.g. Fry

322 1927), is the extremely penetrative type of hyphal bundles associated with the occurrence of
323 apothecia, which are able to reach much deeper into the schist than adjacent hyphae (Fig. 1).
324 Analysis of the effects of penetrating hyphae have long been relying on the use of scanning
325 electron microscopy (SEM) and other high-resolution laboratory techniques (e.g. Jones *et al*.
326 1981, Strech & Viles 2002, Wierzchos & Ascaso 1994). Although extremely useful for
327 examining the very specific changes occurring in rock minerals by direct contact with individual
328 hyphae, the scale of these approaches is often too small to answer questions related with the
329 performance of the entire lichen or lichen community at the scale of the whole surface (micro-
330 scale) or site where these surfaces are located (meso-scale). Additionally, these techniques may
331 only be considering worst (or best) case scenarios resulting from chance unless they are based on
332 large sample sizes and use full random sampling as in Strech & Viles (2002) to achieve statistical
333 robustness.
334 Many studies have determined the maximum or average depth of hyphal penetration for a wide
335 range of lithotypes, but usually ignore hyphal spread, with few exceptions (Bartoli et al. 2014,
336 Casanova-Municchia et al. 2014, Gazzano et al. 2009a). Image analysis of colonized cross-
337 sections after PAS staining retrieved accurate values for the hyphal spread of each species inside
338 the rock (Table 1; Fig. 1). These values could then be used to determine if surface orientation
339 had any effect on species ability to spread into the rock interior and induce mineral breakdown.
340
341 [Fig. 1 approximately here]
342
343 The studied lichens differed significantly in the spread of the HPC irrespective of surface
344 orientation (F-value= 10.974, p-value< 0.001). These differences were caused by a significantly

345 higher hyphal spread in *Lecanora pseudistera* than in any other of the lichens analysed, whereas
346 *Aspicilia hoffmanniana*, *Caloplaca subsoluta* and *Peltula euploca* were very similar among each
347 other (Table 1). The effect of interaction between species and surface orientation was not
348 statistically significant (F-value= 0.867, p-value= 0.364) neither was the effect of orientation
349 itself (F-value= 1.339, p-value= 0.262), which means that even if there were differences between
350 species in terms of their ability to spread inside the rock, there are no statistically significant
351 differences between NW and SE oriented surfaces in any of the studied species.
352
353 Weathering is quite obvious to the naked eye in most samples, where the black to more usually
354 dark-grey rock core corresponding to unweathered parent rock gradually changes into the light
355 brown to greyish-brown coloured weathering rind (Fig. 1b). All samples from NW facing
356 surfaces showed such features, against only 13% of the samples from SE facing surfaces. The
357 dimension of the weathering rind was unrelated with the extent of the HPC (Table 1: Spearman=
358 – 0.012).
359
360 [Table 1 approximately here]
361
362 Although the extent of the HPC is unrelated to surface orientation, as species differ in their
363 ability to spread inside the rock, an indirect effect of orientation on lichen-induced physical
364 weathering, as depicted by the proxy HPC, could be produced by means of the abundance of
365 individual species. Since *Lecanora pseudistera* is the most effective in terms of hyphal spread
366 among the four lichens analysed (Table 1), and having been the most frequent and abundant on
367 NW facing slopes (Marques *et al*. 2014) one might assume a more intensive lichen-induced

368 physical weathering happening at NW than at SE facing surfaces in the Côa Valley. Among the
369 four lichens analysed, *Peltula euploca* was probably the most surprising in terms of physical
370 performance since the attachment of this peltate (shield-like) growth form is far from being
371 limited to superficial layers, penetrating up to 3.9 mm into the rock.
372
373 Lichen-induced chemical weathering
374
375 FT-Raman and complementary X-ray microdiffraction analyses of bare-rock controls confirmed
376 the presence of quartz, chlorite, muscovite and albite as the major minerals in all analysed
377 locations of the presumably unweathered schist (Fig. 2 and Supporting Information Tables S1
378 and S2).
379
380 [Fig. 2 approximately here]
381
382 The wavenumber region 100-1700 cm^{-1} of FT-Raman spectra contains useful spectroscopic
383 information about metabolic by-products of the lichen-induced weathering process (Edwards *et*
384 *al.* 1995, Jorge-Villar *et al.* 2004).
385 Phyllosilicates and quartz are the strongest features in the internal layers of all lichen-colonized
386 samples (Fig. 2), corresponding well with the presumably unweathered parent rock type.
387 Phyllosilicates have complex structures and highly variable compositions (Wang *et al.* 2002)
388 reflected in complex FT-Raman spectra, but for the purpose of this paper, the occurrence of
389 phyllosilicates can be usefully discussed in terms of the 100-600 cm^{-1} spectral region, where,
390 contrary to what happens in other regions of the spectra, peaks related to phyllosilicates are

391 easier to differentiate from those related to other substances (see below). According to Wang *et*
392 *al.* (2002) di-octahedral phyllosilicates such as muscovite produce a strong FT-Raman peak at
393 260 cm^{-1}, which is depicted in the FT-Raman spectra of the rock interior and lichen-rock
394 interface of almost all colonized samples. Mg-bearing phyllosilicates, such as chlorite, peak
395 strongly at approximately 350 cm^{-1}. The peak at 356 cm^{-1} visible in the FT-Raman spectra of the
396 rock interior and lichen-rock interface of schist samples colonized by *Aspicilia hoffmanniana*
397 (Fig. 2), can therefore be assigned to chlorite. Peaks at 200 cm^{-1} are characteristic of tri-
398 octahedral phyllosilicates (Wang *et al.* 2002) and most probably indicate the presence of either
399 chlorite or biotite. Quartz is very resistant to weathering and persists even at the surface of bare
400 rock and at the lichen-rock interface of all samples (Fig. 2). It was detected in every sample by a
401 sharp band at 464 cm^{-1} in FT-Raman spectra and at 3.33 Å in X-ray microdiffraction (Supporting
402 Information Tables S1 to S10). The presence of the same band in the FT-Raman spectra of
403 *Aspicilia hoffmanniana* and *Caloplaca subsoluta* (Fig. 2a) indicates an incorporation of quartz
404 particles by the thallus of these lichens. Evidence for the ability of *Aspicilia hoffmanniana* to
405 incorporate phyllosilicate particles is also seen in its FT-Raman spectra, with characteristic bands
406 at 200 and 260 cm^{-1} (Wang *et al*. 2002). However, the occurrence of quartz and phyllosilicates in
407 lichen thalli and lichen-rock interfaces can also have an exogenous origin from airborne dust, as
408 suggested by Vingiani *et al.* (2013) after detecting the same kind of mineral incorporation in
409 lichens growing on quartz- and phyllosilicate-free vulcanic rocks. Incorporation of quartz and
410 phyllosilicate minerals by lichens is not exclusive of crustose lichens as can be inferred by the
411 FT-Raman spectra of *Peltula euploca* showing a band at 432 cm^{-1} (Fig 3), which is assignable to
412 either of these silicate minerals. This would require further confirmation through higher
413 resolution techniques such as scanning electron microscopy (SEM).

414 Besides those minerals that are known to characterize the unweathered rock (see materials and
415 methods section), X-ray microdiffraction and FT-Raman spectroscopy confirmed the occurrence
416 of halloysite at both the virtual interface of bare rock samples and the lichen-rock interfaces,
417 irrespective of the species and the orientation of the parent outcrop (Figs 2). Halloysite is a
418 common product of schist weathering, resulting from the transformation of chlorite, biotite,
419 muscovite and feldspars (Banfield & Eggleton 1990, Kretzschmar et al. 1997, Parham 1969).
420 Despite the differences stated above in terms of weathering rind formation, no differences were
421 observed in terms of the occurrence of halloysite between NW and SE facing surfaces. Peak at
422 260 cm^{-1} in FT-Raman spectra could also correspond to kaolinite, another product of schist
423 weathering, but differentiation of kaolinite minerals from muscovite, and the latter from
424 vermiculite, can be problematic because peaks shared by the three minerals are not fully
425 differentiable by X-ray microdiffraction or FT-Raman spectroscopy (Wang et al. 2002).
426
427 FT-Raman and complementary X-ray microdiffraction analyses also allowed detecting the
428 occurrence of neoformation minerals commonly attributed to lichen activity, namely calcium
429 oxalates, at the lichen-rock interface and thalli of some of the target species, and confirmed their
430 absence at the rock interior of all samples. The pattern of occurrence of such minerals is,
431 however, variable among the considered species, their origin and analysed location within
432 samples.
433 Key molecular signatures for oxalates occur in the 1400-1500 cm^{-1} region of FT-Raman spectra
434 (Edwards *et al.* 2003b) where 1476 cm^{-1} is considered distinctive for weddellite (Fig. 2b). Other
435 distinguishing bands for weddellite occur at 912 and 1634 cm^{-1}. The signature of weddellite was
436 found either completely or partially in the thalli of *Aspicilia hoffmanniana*, *Lecanora pseudistera*

437 and *Peltula euploca* from south-east facing surfaces (Fig 3a), but not in the thalli of *Caloplaca*
438 *subsoluta* neither in any of the specimens taken from north-west facing surfaces (Fig 2a). In fact,
439 previous experimental works had indicated that microclimatic factors could be important in
440 determining the state of hydration of calcium oxalate in lichens (Edwards *et al.* 1995) and have
441 associated the occurrence of the dyhidrate form with lichen's strategy for maintaining its water
442 balance in dry exposed surfaces (Prieto *et al*. 2000, Prieto & Silva 2003).
443 Calcium oxalate monohydrate, known as whewellite, has been detected in the thalli of *Aspicilia*
444 *hoffmanniana* and *Lecanora pseudistera* on samples from NW facing surfaces, peaking in FT-
445 Raman spectra at 1463 and 1631 cm^{-1}, respectively (Fig. 2).
446 Variation in measured temperature and relative humidity between NW and SE facing surfaces is
447 summarized in Table 2. There are similarities in the general pattern of annual rock surface
448 temperature and relative humidity regimes. Both NW and SE facing surfaces exhibited a
449 seasonal pattern of high temperature and low relative humidity values from around June to
450 September followed by a much colder and moist period between November and February.
451 Variation in temperature was huge at both orientations, but nevertheless higher at SE than at NW
452 facing surfaces. The same happened with relative humidity, although relative humidity was
453 always higher at NW facing surfaces than at SE facing surfaces.
454 The occurrence of oxalates in the lichen thallus of *Aspicilia hoffmanniana* and *Lecanora*
455 *pseudistera* is not completely unexpected since the fruiting bodies of the former are well known
456 for being pruinose (*i.e.* covered by oxalate crystals) and the later belongs to a group of lichens
457 that are characterized precisely by the presence of large amphithecial crystals. The occurrence of
458 the monohydrate form in specimens that grow under less contrasting humidity and temperature
459 regimes is consistent with the physiological role attributed to calcium oxalate.

460 The origin of Ca ions for calcium oxalate production in lichens, however, is still an unsolved
461 matter. Calcite ($CaCO_3$) is usually present in the matrix of the studied rock type in sufficient
462 amounts to produce effervescence when treated with dilute hydrochloric acid. Calcite is highly
463 alterable and a potential source of Ca ions for calcium oxalate formation promoted by biological
464 colonization. However, calcite, with characteristic features in FT-Raman spectra being a strong,
465 sharp band at 1086 and weaker bands at 712 and 286 cm^{-1} (Edwards *et al.* 1995, 2003b), is
466 missing in all schist samples.
467 Although it has been proved that lichens are able to uptake Ca ions from calcareous rocks such
468 as limestones and marbles for calcium oxalate production (*e.g.* Seaward & Edwards 1995), the
469 rock is definitely not the only source of this element as the occurrence of both forms of calcium
470 oxalate has been reported in lichens colonizing non-calcareous substrates such as granites (e.g.
471 Prieto & Silva 2003), serpentinites (Favero-Longo et al. 2005) or even tree-bark (Edwards et al.
472 2005) and tree leafs (de Oliveira et al. 2002). The presence of calcium oxalates inside the lichen
473 thallus is therefore not necessarily indicative of its biodeteriogenic activity and, when the
474 calcium source is exogenous, calcium oxalate patinas were even indicated as bioprotective
475 (McIlroy de la Rosa et al. 2013). Occurrence of calcium oxalates in lichens growing on iron- and
476 magnesium-rich siliceous rocks instead of the most expected ferrous oxalate dehydrate
477 (humboldtine) and magnesium oxalate (glushinskite), respectively, has also been reported before
478 (e.g. Prieto et al. 1997, 2000, Prieto & Silva 2003, Favero-Longo et al. 2005). This phenomenon
479 can, according to Prieto & Silva (2003) and Favero-Longo et al. (2005), be explained by the
480 higher water solubility of ferrous and magnesium oxalates as well as their higher susceptibility to
481 oxidation. The detection of calcium oxalates at the lichen-rock interface by X-ray
482 microdiffraction (Table 3 and Supporting Information Table S7, S9 and S10), however, is not as

483 easily assignable to external sources of Ca. Only weddellite has been detected at the lichen-rock
484 interface and that was by X-ray microdiffraction exclusively on samples taken from SE facing
485 surfaces, colonized by *Caloplaca subsoluta*, *Lecanora pseudistera* and *Peltula euploca* (Table
486 3). Weddellite was apparently absent from the lichen-rock interface of *Aspicilia hoffmanniana*
487 although present in the thallus (Table 4). The opposite was observed in the samples colonized by
488 *Caloplaca subsoluta*, with weddellite detected at the lichen-rock interface by X-ray
489 microdiffraction (Table 3) and no form of calcium oxalate detected inside the thallus by FT-
490 Raman (Table 4). These results suggest that calcium oxalates at the lichen-rock interface and
491 inside the lichen thallus may have different origins and/or functions. Except for the occurrence of
492 weddellite, FT-Raman spectroscopy and X-ray microdiffraction of the lichen-rock interface
493 retrieved quite similar results to that of the virtual interface in bare rock controls.
494 The relevance of these results in the search for the causes of differential weathering of schist
495 surfaces in the Côa Valley is opposite to those already mentioned for lichen-induced physical
496 weathering. Assuming that calcium oxalate at the lichen-rock interface is being produced from
497 Ca taken from the rock and considering its formation as a proxy of lichen-induced chemical
498 weathering, such type of weathering might be more intense on SE facing surfaces. The
499 possibility that due to differences in micro-environmental conditions, calcium oxalates on SE
500 surfaces are subject to less dissolution and are consequently more stable than those on NW
501 surfaces cannot be ruled out by present evidence. However it seems unlikely because the poorly
502 soluble Ca oxalates were found to persist at the lichen-rock interface of thalli exposed to
503 significantly higher precipitation regimes (Favero-Longo et al. 2005).
504 Other bands present in FT-Raman spectra include 1158, 1552 and 1612 cm^{-1}, which are
505 characteristic of parietin and therefore present in the FT-Raman spectra of *Caloplaca subsoluta*.

506 The resemblance of the FT-Raman spectra of *Caloplaca subsoluta* and that of other members of
507 the lichen family Teloschistales (Jorge-Villar *et al.* 2004) is quite obvious mainly due to the
508 profile of parietin.
509 The FT-Raman spectra of the thallus of *Aspicilia hoffmanniana* and *Lecanora pseudistera* on
510 samples taken from NW and SE facing surfaces, respectively, contain a series of bands that
511 could not be assigned to any substance for the time being, but are probably related with other
512 secondary metabolites produced by these lichens, which may further act as biodeteriogenic
513 factors (Adamo & Violante 2000, with refs. therein). Also unknown were the peaks at 5.96 and
514 9.09 Å in X-ray microdiffraction of samples colonized by *Aspicilia hoffmanniana* and 2.32 Å in
515 samples colonized by *Aspicilia hoffmanniana* and *Caloplaca subsoluta* (Supporting Information
516 Table S7 and S9). The very broad bands at 1332 and 1595 cm^{-1} of all FT-Raman spectra are due
517 to amorphous carbon.
518
519 **Conclusions**
520
521 Variation in microclimatic factors related to surface orientation produces different effects
522 depending on the nature of lichen-induced weathering. Analysis of stained polished cross-
523 sections of schist samples colonized by the crustose *Aspicilia hoffmanniana*, *Caloplaca*
524 *subsoluta*, *Lecanora pseudistera* and the squamulose *Peltula euploca* showed that hyphae
525 originating from the medulla of these lichens penetrate more than 30 mm and follow a
526 unidirectional pattern along the depth rock profile. The lamellar nature of schist minerals
527 offering pathways of least resistance along intermineral voids, probably favours this deep
528 penetration. Therefore the effects of hyphal penetration on schist should go far beyond the

surface and also involve the minerals in the deeper layers. The spread of the hyphal penetration component in the analysed species was similar on NW and SE facing surfaces, but may turn out to be more severe at NW facing surfaces, due to the higher frequency and abundance of species with higher penetrative ability, such as *Lecanora pseudistera*. Orientation is thus likely to have an indirect effect on lichen-induced physical weathering by means of the abundance patterns of individual species, highlighting the importance of accurate estimates of the relative abundances of colonizing species, stemming from community ecology approaches, for rock-art condition assessments.

Other evidences of lichen-induced weathering produced in these rocks are related with the incorporation of quartz and phyllosilicate particles by the thalli of all the lichens studied, including the squamulose *Peltula euploca*. The external origin of these particles cannot be ruled out, however, as the mechanisms of airborne mineral incorporation by the lichen thallus are not fully understood. Also of interest for the purpose of this study is the presence of kaolinite and halloysite, two common products of schist weathering, at the lichen-rock interface and on the surface of bare rock controls, irrespective of surface orientation. Variations in the amount of these minerals depending on the colonizing species and microclimatic factors remain to be tested.

Evidence for the occurrence of metabolic by-products of lichen activity in the analysed samples is limited to calcium oxalates. Specimens of *Aspicilia hoffmanniana* from dry SE facing surfaces produced weddellite exclusively, while those from moist NW facing surfaces produced a mixture of weddellite and whewellite. Specimens of *Lecanora pseudistera* produced weddellite on SE facing surfaces and whewellite on NW facing surfaces. Weddellite was also detected inside the thalli of squamulose *Peltula euploca*, occurring only on SE facing surfaces. None of these forms

552 of calcium oxalate were detected inside the thalli of *Caloplaca subsoluta*. These results indicate,
553 as others beforehand, that there is some preference among the studied lichens for the production
554 of the dehydrate form of calcium oxalate under the highly variable microclimate conditions
555 provided by SE facing surfaces, while on the slightly less variable NW facing surfaces, a mixture
556 of both monohydrate and dehydrate forms can occur. Given the possibility of calcium uptake
557 from airborne particles, it is impossible to state unequivocally whether calcium ions used in the
558 formation of calcium oxalates were acquired from the substrate, but the probability that this
559 might have happened is higher in those cases where calcium oxalates were also detected at the
560 lichen-rock interface. Weddellite was detected at the interface of all species except *Aspicilia*
561 *hoffmanniana* from SE facing surfaces.
562 This study therefore suggests that lichen-induced physical weathering in the Côa Valley is
563 species-specific and may be stronger on north-east facing surfaces, whereas lichen-induced
564 chemical action is microclimatically controlled and may be more severe on SE facing surfaces.
565 There is probably some variation in the relative abundance of alteration minerals and calcium
566 oxalates at different portions of the samples but according to present evidence, the lichens
567 currently dominant on the vertical schist surfaces in the Côa Valley are unlikely to be responsible
568 for the differential weathering (and presumably consequent distribution pattern) of engraved
569 schist surfaces.
570 Furthermore, calcium oxalate production by lichens not attributable to any kind of lichen
571 activity, as it happens with *Aspicilia hoffmanniana*, adds to the doubts concerning its importance
572 in lichen-induced weathering, especially since this seems to be limited to a few species, and, as
573 demonstrated by this study, changes with microclimatic conditions. Assumptions about the
574 drivers of open-air rock-art distribution elsewhere should therefore also consider the micro-

environmental controls of lichen-induced weathering and associated deteriogenic activity in order to avoid biased measures of the influence of lichen activity in the deterioration process, or superficial decisions in terms of rock-art conservation practices.

Acknowledgements

The authors are grateful to the Côa Valley Archaeological Park for permission to collect lichen specimens. The archaeologists Thierry Aubry and Luis Luis are specially acknowledge for valuable information on the location of sampling sites and for raising the questions that motivated this study. Pio González and Pablo Barreiro (University of Vigo) are gratefully acknowledged for providing detailed methodological guidance and relevant suggestions for the improvement of some laboratory procedures. The first author was supported by Fundação para a Ciência e Tecnologia (FCT) through PhD grant SFRH/BD/42248/2007. The study was partially financed by Fundo do Baixo Sabor para Biodiversidade through and by the European Regional Development Fund (ERDF) through the Spanish Ministry of Science and Innovation under the project CGL2011-22789.

Literature cited

Adamo P., Violante P. (2000) Weathering of rocks and neogenesis of minerals associated with lichen activity. *Applied Clay Science* 16, 229-256.

596 Adamson C., McCabe S., Warke P.A., McAllister D., Smith B.J. (2013) The influence of aspect
597 on the biological colonization of stone in Northern Ireland. *International Biodeterioration*
598 *and Biodegradation* 84, 357-366.
599 Aghamiri R., Schwartzman D.W. (2002) Weathering rates of bedrock by lichens, a mini
600 watershed study. *Chemical Geology* 188, 249-259.
601 Aires S., Carvalho C., Noronha F., Ramos J.F., Moura C., Sant'Ovaia H., Sousa M. (2011) Os
602 xistos do complexo xisto-grauváquico – grupo do Douro. Potencial como recurso
603 geológico. In *Actas do VI Seminário Recursos Geológicos, Ambiente e Ordenamento do*
604 *Território*, Vila Real, 6-8 October 2011, pp. 159-165. UTAD, Vila Real.
605 Arocena J.M., Siddique T., Thring R.W., Kapur S. (2007) Investigation of lichens using
606 molecular techniques and associated mineral accumulations on a basaltic flow in a
607 Mediterranean environment. *Catena* 70, 356-365.
608 Ascaso C., Galvan J., Ortega C. (1976) The pedogenic action of *Parmelia conspersa*,
609 *Rhizocarpon geographicum* and *Umbilicaria pustulata*. *The Lichenologist* 8, 151-171.
610 Aubry T., Luís L., Dimuccio L.A. (2012) Nature vs. Culture, present-day spatial distribution and
611 preservation of open-air rock-art in the Côa and Douro River Valleys (Portugal). *Journal of*
612 *Archaeological Science* 39 (4), 848-866.
613 Banfield J.F., Eggleton R.A. (1990) Analytical transmission electron microscope studies of
614 plagioclase, muscovite, and K-feldspar weathering. *Clays and Clay Minerals* 38 (1), 77-89.
615 Bartoli F., Municchia A.C., Futagami Y., Kashiwadani H., Moon K.H., Caneva G. (2014)
616 Biological colonization patterns on the ruins of Angkor temples (Cambodia) in the
617 biodeterioration vs bioprotection debate. *International Biodeterioration and*
618 *Biodegradation* 96, 157-165.

619 Boulesteix A.-L., Janitza S., Kruppa J., König I.R. (2012) Overview of Random Forest
620 methodology and practical guidance with emphasis on computational biology and
621 bioinformatics. *Wiley Interdisciplinary Reviews, Data Mining and Knowledge Discovery* 2,
622 493-507.
623 Breiman L. (2001) Random Forests. *Machine Learning* 45, 5-32.
624 Búrcio M. (2004) Controle estrutural da localização de pedreiras de esteios de xisto para vinha
625 em Vila Nova de Foz Côa. MSc Thesis. University of Évora.
626 Caneva G. (1993) Ecological approach to the genesis of calcium oxalate patinas on stone
627 monuments. *Aerobiologia* 9, 149-156.
628 Cann J.H. (2012) Physical weathering of slate gravestones in a Mediterranean climate.
629 *Australian Journal of Earth Sciences* 59 (7), 1021-1032.
630 Carballal R., Paz-Bermúdez G., Sánchez-Biezma M.J., Prieto B. (2001) Lichen colonization of
631 coastal churches in Galicia, biodeterioration implications. *International Biodeteriorarion*
632 *and Biodegradation* 47, 157-163.
633 Carter N.E.A., Viles H.A. (2003) Experimental investigations into the interactions between
634 moisture, rock surface temperatures and an epilithic lichen cover in the bioprotection of
635 limestone. *Building and Environment* 38 (9-10), 1225-1234.
636 Carter N.E.A., Viles H.A. (2005) Bioprotection explored: the story of a little known earth surface
637 process. *Geomorphology* 67 (3), 273-281.
638 Casanova Municchia A., Percario Z., Caneva G. (2014) Detection of endolithic spatial
639 distribution in marble stone. *Journal of Microscopy* 256 (1), 37-45.
640 Chen J., Blume H.P., Beyer L. (2000) Weathering of rocks induced by lichen colonization - a
641 review. *Catena* 39 (2), 121-146.

642 de Mendiburu F. (2013) agricolae, statistical procedures for agricultural research. R package
643 version 1.1-5.
644 de Oliveira L.F.C., Edwards H.G.M., Feo-Manga J.C., Seaward M.R.D., Lücking R. (2002) FT-
645 Raman spectroscopy of three foliicolous lichens from Costa Rican rainforests. *The*
646 *Lichenologist* 34 (3), 259-266.
647 Edwards H.G.M., Garcia-Pichel F., Newton E.M., Wynn-Williams D.D. (2000) Vibrational
648 Raman spectroscopic study of scytonemin, the UV-protective cyanobacterial pigment.
649 *Spectrochimica Acta Part A* 56 (1), 193-200.
650 Edwards H.G.M., Newton E.M., Wynn-Williams D.D., Lewis-Smith R.I. (2003a) Non-
651 destructive analysis of pigments and other organic compounds in lichens using Fourier-
652 transform Raman spectroscopy: a study of Antarctic epilithic lichens. *Spectrochimica Acta*
653 *Part A* 59, 2301-2309.
654 Edwards H.G.M., Russell N.C., Seaward M.R.D. (1997) Calcium oxalate in lichen
655 biodeterioration studied using FT-Raman spectroscopy. *Spectrochimica Acta Part A* 53,
656 99-105.
657 Edwards H.G.M., de Oliveira L.F.C., Seaward M.R.D. (2005) FT-Raman spectroscopy of the
658 Christmas wreath lichen, *Cryptothecia rubrocincta* (Ehrenb.,Fr.) Thor. *The Lichenologist*
659 37 (2), 181-189.
660 Edwards H.G.M., Russell N.C., Seaward M.R.D., Slarke D. (1995) Lichen biodeterioration
661 under different microclimates, an FT Raman spectroscopic study. *Spectrochimica Acta*
662 *Part A* 51, 2091-2100.

663 Edwards H.G.M., Seaward M.R.D., Attwood S.J., Little S.J., de Oliveira L.F.C., Tretiach M.
664 (2003b) FT-Raman spectroscopy of lichens on dolomitic rocks, an assessment of metal
665 oxalate formation. *The Analyst* 128, 1218-1221.
666 Favero-Longo S.E., Castelli D., Salvadori O., Belluso E., Piervittori R. (2005) Pedogenetic
667 action of the lichens *Lecidea atrobrunnea*, *Rhizocarpon geographicum* gr. and *Sporastatia*
668 *testudinea* on serpentinized ultramafic rocks in an alpine environment. *International*
669 *Biodeterioration and Biodegradation* 56 (1), 17-27.
670 Favero-Longo S.E., Gazzano C., Girlanda M., Castelli D., Tretiach M., Baiocchi C., Piervittori
671 R. (2011) Physical and Chemical Deterioration of Silicate and Carbonate Rocks by
672 Meristematic Microcolonial Fungi and Endolithic Lichens (Chaetothyriomycetidae).
673 *Geomicrobiology Journal* 28 (8), 732-744.
674 Fernandes A.P.B. (2012) Natural processes in the degradation of open-air rock-art sites: an
675 urgency intervention scale to inform conservation. PhD Dissertation. Bournemouth
676 University.
677 Freeman J.J., Wang A., Kuebler K.E., Jolliff B.L., Haskin L.A. (2008) Characterization of
678 natural feldspars by Raman spectroscopy for future planetary exploration. *The Canadian*
679 *Mineralogist* 46, 1477-1500.
680 Frost (1997) The structure of the kaolinite minerals – a FT-Raman study. *Clay Minerals* 32, 65-
681 77.
682 Fry E.J. (1924) A suggested explanation of the mechanical action of lithophytic lichens on rock
683 (shale). *Annals of Botany* 38, 175-196.
684 Fry E.J. (1927) The mechanical action of crustaceous lichens on substrate of shale, schist, gneiss,
685 limestone and obsidian. *Annals of Botany* 41, 437-460.

686 Galvan J., Rodriguez C., Ascaso C. (1981) The pedogenic action of lichens in metamorphic
687 rocks. *Pedobiologia* 21, 60-73.
688 Gazzano C., Favero-Longo S.E., Matteucci E., Piervittori R. (2009a) Image analysis for
689 measuring lichen colonization on and within stonework. *The Lichenologist* 41 (3), 299-
690 313.
691 Gazzano C., Favero-Longo S.E., Matteucci E., Roccardi A., Piervittori R. (2009b) Index of
692 lichen potential biodeteriogenic activity (LPBA), a tentative tool to evaluate the lichen
693 impact on stonework. *International Biodeterioration and Biodegradation* 63 (7), 836-843.
694 Giordani P., Modenesi P., Tretiach M. (2003) Determinant factors for the formation of the
695 calcium oxalate minerals, weddellite and whewellite, on the surface of foliose lichens. *The*
696 *Lichenologist* 35 (3), 255-270.
697 Gomes L. M. F., Almeida P. G. (2003) As pedreiras do Poio (Foz Côa) - a região e o turismo. In
698 *A Geologia de Engenharia e os Recursos Geológicos. Vol. 1. Geologia de Engenharia* (ed
699 M.P.V. Ferreira), pp. 299-316. Imprensa da Universidade de Coimbra, Coimbra.
700 Jones D., Wilson M.J., McHardy W.J. (1981) Lichen weathering of rock-forming minerals,
701 application of scanning electron microscopy and microprobe analysis. *Journal of*
702 *Microscopy* 124, 95-104.
703 Jorge-Villar S.E., Edwards H.G.M., Seaward M.R.D. (2004) Lichen biodeterioration of
704 ecclesiastical monuments in northern Spain. *Spectrochimica Acta Part A* 60, 1229-1237.
705 Kidron G.J., Temina M. (2010) Lichen colonization on cobbles in the Negev Desert following 15
706 years in the field. *Geomicrobiology Journal* 27 (5), 455-463.

707 Kretzschmar R, Robarge W.P., Amoozegar A., Vepraskas M.J. (1997) Biotite alteration to
708 halloysite and kaolinite in soil-saprolite profiles developed from mica schist and granite
709 gneiss. *Geoderma* 75 (3-4), 155-170.
710 Liaw A., Wiener M. (2002) Classification and regression by Random Forest. *R News* 2, 18-22.
711 Marques J., Hespanhol H., Paz-Bermúdez G., Almeida R. (2014) Choosing between sides in the
712 battle for pioneer colonization of schist in the Côa Valley Archaeological Park, a
713 community ecology perspective. *Journal of Archaeological Science* 45, 196-206.
714 McIlroy de la Rosa J.P., Warke P.A., Smith B.J. (2013) Lichen-induced biomodification of
715 calcareous surfaces: bioprotection versus biodeterioration. *Progress in Physical Geography*
716 37 (3), 325-351.
717 McIlroy de la Rosa J.P., Warke P.A., Smith B.J. (2014) The effects of lichen cover upon the rate
718 of solutional weathering of limestone. *Geomorphology* 220, 81-92.
719 Oppel S., Strobl C., Huettmann F. (2009) Alternative methods to quantify variable importance in
720 ecology. Technical Report Number 65. University of Munich, Munich.
721 Parham W.E. (1969) Formation of halloysite from feldspar, low temperature, artificial
722 weathering versus natural weathering. *Clays and Clay Minerals* 17, 13-22.
723 Polzehl J., Tabelow K. (2007) Adaptive smoothing of digital images, the R package adimpro.
724 *Journal of Statistical Software* 19, 1-17.
725 Prieto B., Edwards H.G.M., Seaward M.R.D. (2000) A Fourier transform-Raman spectroscopic
726 study of lichen strategies on granite monuments. *Geomicrobiology Journal* 17, 55-60.
727 Prieto V.B., Silva B. (2003) Neoformed calcium minerals in granite colonised by lichens. *Nova*
728 *Acta Científica Compostelana (Bioloxía)* 13, 35-45.

729 Prieto B., Silva B., Rivas T., Wierzchos J., Ascaso C. (1997) Mineralogical transformation and
730 neoformation in granite caused by the lichens *Tephromela atra* and *Ochrolechia parella*.
731 *International Biodeterioration and Biodegradation* 40 (2-4), 191-199.
732 Sanders W.B., Ascaso C., Wierzchos J. (1994) Physical interactions of two rhizomorph-forming
733 lichens with their rock substrate. *Botanica Acta* 107 (6), 432-439.
734 Seaward M.R.D. (1997) Major impacts made by lichens in biodeterioration processes.
735 *International Biodeterioration and Biodegradation* 40 (2-4), 269-273.
736 Seaward M.R.D., Edwards H.G.M. (1995) Lichen-substratum interface studies, with particular
737 reference to Raman microscopic analysis. 1. Deterioration of works of art by *Dirina*
738 *massiliensis* forma *sorediata*. *Cryptogamic Botany* 5 (3), 282-287.
739 Seaward M.R.D. (2015) Lichens as agents of Biodeterioration. In Recent advances in
740 Lichenology. Modern methods and approaches in biomonitoring and bioprospection (eds
741 D.K. Upreti, P.K. Divakar, V. Shukla & R. Bajpai), pp. 189-211. Springer India, New
742 Delhi.
743 Sousa M.B. (1982) Litostratigrafia e estrutura do complex xisto-grauváquico ante-Ordovícico –
744 grupo do Douro (nordeste de Portugal). PhD thesis. University of Coimbra.
745 St. Clair L.L., Seaward M.R.D. (2004) Biodeterioration of stone surfaces. Kluwer Academic
746 Press, Dordrecht.
747 Steinbauer M., Gohlke A., Mahler C., Schmiedinger A., Beierkuhnlein C. (2013) Quantification
748 of wall surface heterogeneity and its influence on species diversity at medieval castles -
749 implications for the environmentally friendly preservation of cultural heritage. *Journal of*
750 *Cultural Heritage* 14 (3), 219-228.

751 Stretch R., Viles H.A. (2002) Lichen weathering on Lanzarote lava flows. *Geomorphology* 47,
752 87-94.
753 Viles H.A., Cutler N.A. (2012) Global environmental change and the biology of heritage
754 structures. *Global Change Biology* 18(8), 2406-2418.
755 Vingiani S., Terribile F., Adamo P. (2013) Weathering and particle entrapment at the rock-lichen
756 interface in Italian volcanic environments. *Geoderma* 207-208, 244-255.
757 Wang A., Freeman J., Kuebler K.E. (2002) Raman spectroscopic characterization of
758 phyllosilicates. 33rd Annual Lunar and Planetary Science Conference, March 11-15,
759 Houston (TX), USA.
760 Wierzchos J., Ascaso C. (1994) Application of back-scattered electron imaging to the study of
761 the lichen-rock interface. *Journal of Microscopy* 175 (1), 54-59.
762 Wierzchos J., Ascaso C. (1996) Morphological and chemical features of bioweathered granitic
763 biotite induced by lichen activity. *Clays and Clay Minerals* 44 (5), 652-657.
764 Wierzchos J., Ascaso C. (1998) Mineralogical transformation of bioweathered granitic biotite,
765 studied by HRTEM, evidence for a new pathway in lichen activity. *Clays and Clay*
766 *Minerals* 46 (4), 446-452.
767 Wierzchos J., de los Ríos A., Ascaso C. (2013) Microorganisms in desert rocks: the edge of life
768 on Earth. *International Microbiology* 15 (4), 172-182.
769 Xu Q.-S., Liang Y.-Z., Du Y.-P. (2004) Monte Carlo cross-validation for selecting a model and
770 estimating the prediction error in multivariate calibration. *Journal of Chemometrics*
771 18,112-120.
772

773 **Tables**

774

775

776 **Table 1.** Hyphal penetration: measures taken out of colonized cross-sections after PAS staining.
777 Depth: estimated depth of hyphal penetration in mm; HPC: area occupied by the hyphal
778 penetration component in mm^2; WR: area occupied by the weathering rind in mm^2. The area
779 analysed in each cross-section was 57.5 mm^2. Different letters in brackets indicate statistically
780 significant pair-wise comparisons (p-value< 0.05).

Species	**Aspect**	**Depth (mean ± sd)**	**Depth (max)**	**HPC (mean ± sd)**	**WR**
Aspicilia hoffmanniana	South-east	5.7 ± 7.6	37.0	2.96 ± 2.03 (a)	0.00
	North-west	3.5 ± 3.5	12.0	2.37 ± 0.81 (a)	0.00
Caloplaca subsoluta	South-east	4.1 ± 5.3	30.0	2.09 ± 1.71 (a)	4.07
	North-west	1.8 ± 1.9	6.8	1.74 ± 0.71 (a)	7.56
Lecanora pseudistera	South-east	5.1 ± 6.6	31.0	8.01 ± 2.02 (b)	0.00
	North-west	4.1 ± 3.8	13.0	5.79 ± 2.97 (b)	30.36
Peltula euploca	South-east	2.4 ± 1.0	3.9	0.69 ± 0.60 (a)	6.72
				Spearman: – 0.012	

781
782
783

784 **Table 2.** Data on rock surface microclimate at opposite orientations in the Côa Valley.

		North-west	South-east
Temperature	Average	17 ºC	20 ºC
	Minimum	13 ºC	15 ºC
	Maximum	23 ºC	30 ºC
Relative humidity	Average	70 %	63 %
	Minimum	55 %	45 %
	Maximum	81 %	77 %

785

786

787 **Table 3.** Summary of the neoformed calcium minerals detected in the lichen-rock interface (FT-

788 Raman spectroscopy and X-ray microdiffraction).

	Aspicilia hoffmanniana		*Caloplaca subsoluta*		*Lecanora pseudistera*		*Peltula euploca*
	North-west	South-east	North-west	South-east	North-west	South-east	South-east
Whewellite							
Weddellite				X		X	X

789

790

791 **Table 4.** Summary of the minerals detected in lichen thalli (FT-Raman spectroscopy)

	Aspicilia hoffmanniana		*Caloplaca subsoluta*		*Lecanora pseudistera*		*Peltula euploca*
	North-west	South-east	North-west	South-east	North-west	South-east	South-east
Whewellite	X				X		
Weddellite	X	X				X	X
Quartz		X	X				X
Phyllosilicates		X				X	

792

793 **Figure legends**

794

795 **Figure 1.** On the top, cross-sections of schist samples colonized by *Lecanora pseudistera* from a
796 north-west facing surface (a) and by *Aspicilia hoffmanniana* from a south-east facing surface (b);
797 and on the bottom, cross-section of a schist sample colonized by *Aspicilia hoffmanniana* from a
798 south-east facing surface after PAS staining (c) and respective image classification (d) with
799 medium grey areas corresponding well with the area occupied by the hyphal penetration
800 component (in purple in the original image).

801

802 **Figure 2.** FT-Raman spectra of bare rock control samples (first row) and colonized samples
803 (remaining rows). On the first row: external surface (thick line), internal surface (thin line) and
804 core (dotted line) of bare rock control samples from north-west (a) and south-east (b) facing
805 vertical schist surfaces. On the remaining rows: thallus surface (thick lines), rock-lichen interface
806 (thin lines) and rock core (dotted lines) of, from top to bottom, *Aspicilia hoffmanniana*,
807 *Caloplaca subsoluta*, *Lecanora pseudistera* and *Peltula euploca* from north-west (a) and south-
808 east (b) facing vertical schist surfaces. Conditions as explained in material and methods.
809 Wavenumber region: 100-1700 cm^{-1}. Wavenumber assignments are based on Freeman et al.
810 (2008), Frost (1997), Wang et al. (2002), Jorge-Villar et al. 2004, Edwards et al. (1997, 2000,
811 2003a). Additional information on the wavenumbers for the Raman spectra of all species and
812 respective wavenumber assignment is given in Supporting Information Tables S1-S5.

813

814

815

816

817 **Figure 1**

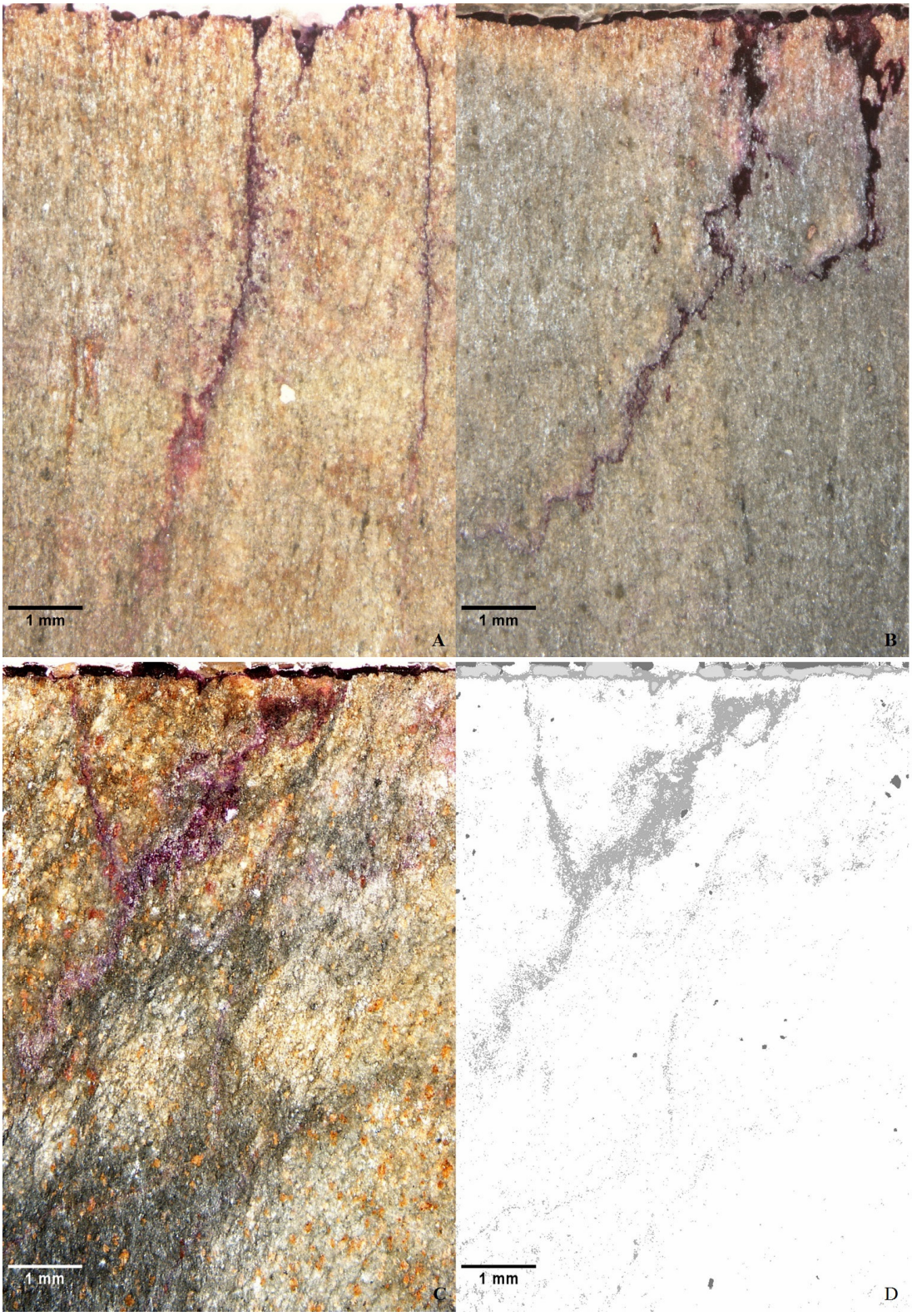

818

Figure 2

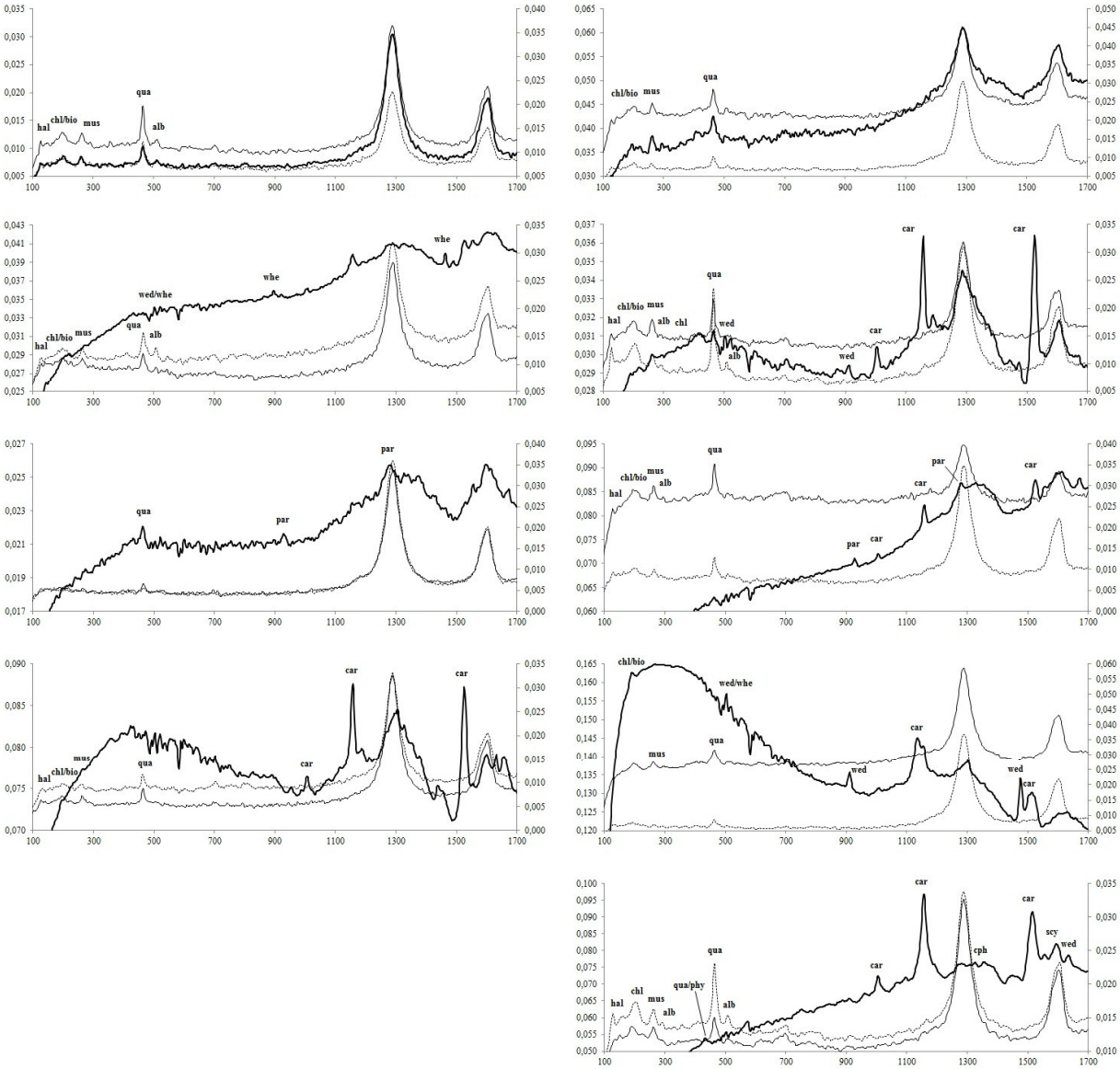
hal
chl/bio
mus
qua
alb
wed/whe
whe
par
car
wed
chl
qua/phy
cph
scy
A
B